

UNIVERSIDAD DE CANTABRIA
ESCUELA TÉCNICA SUPERIOR DE INGENIEROS
INDUSTRIALES Y DE TELECOMUNICACIONES



Departamento de Ingeniería Química y Química Inorgánica

**Contribución al Diseño de Procesos de Separación con
Membranas Líquidas Selectivas. Tratamiento de Aguas
Subterráneas Contaminadas con Cr(VI)**

**Memoria de Tesis Doctoral presentada para optar al
Título de Doctor por la Universidad de Cantabria**

EUGENIO BRINGAS ELIZALDE

DIRECTORAS DE TESIS:

DRA. INMACULADA ORTIZ URIBE

DRA. M^a FRESNEDO SAN ROMÁN SAN EMETERIO

SANTANDER, ABRIL 2008

5. CONCLUSIONES FINALES

El objetivo global de esta Tesis Doctoral ha sido el desarrollo de la metodología de diseño óptimo de un proceso de separación-concentración con membranas líquidas selectivas aplicado a la separación de mezclas multicomponente, con recuperación selectiva del componente de interés. Como caso de estudio se ha investigado la separación selectiva y concentración de cromo(VI) presente inicialmente en un acuífero subterráneo contaminado por acción de la actividad industrial desarrollada a nivel superficial y donde a su vez, coexisten otras especies aniónicas competitivas (sulfato y cloruro mayoritariamente) presentes por las propias características del acuífero y por su localización en una zona litoral. El estudio se ha desarrollado empleando la tecnología de pertracción en emulsión (EPT) en contactores de fibras huecas, considerada como una alternativa innovadora que permite superar las limitaciones o inconvenientes de otras configuraciones basadas en la tecnología de extracción con disolventes en contactores de membrana.

La metodología de diseño propuesta parte del análisis y caracterización del sistema de extracción-reextracción como etapa previa al estudio cinético y modelado matemático del proceso de separación-concentración el cual, es una herramienta imprescindible en la etapa de diseño donde se aplican técnicas de optimización matemática para la determinación de la configuración óptima del proceso que permita alcanzar los objetivos de separación y concentración, con el mínimo coste.

A partir de los resultados obtenidos en los diferentes capítulos de esta Tesis Doctoral se pueden enumerar las siguientes conclusiones parciales:

1. Caracterización y Análisis del Sistema de Extracción-Reextracción (Capítulo 2)

Caracterización del efluente problema

- Con el fin de evitar la posible precipitación en los contactores de membrana, del calcio presente en las aguas subterráneas, el estudio se llevó a cabo con disoluciones a pH ácido trabajando con los aniones mayoritarios (cromo(VI), sulfato y cloruro) del efluente de partida en los intervalos de

concentración: cromo(VI), 9,6-26 mol/m³; sulfato, 10-29 mol/m³; cloruro, 10-33 mol/m³.

Selección de los agentes de extracción y reextracción

- A partir de la información obtenida de la bibliografía, se seleccionaron Alamine 336 (amina terciaria) y NaOH como agentes extractante y reextractante, respectivamente.

Análisis de la co-extracción de especies competitivas

El análisis de la co-extracción de las especies competitivas (sulfato y cloruro) se llevó a cabo mediante una planificación de experimentos de extracción en sistema rotatorio variando la concentración inicial de cromo(VI) para tres tipos de sistemas: i) binario con cromo y sulfato, ii) binario con cromo y cloruro y iii) ternario con cromo, sulfato y cloruro, obteniendo las siguientes conclusiones,

- El porcentaje de extracción de cromo es independiente de la presencia de sulfato y cloruro.
- El porcentaje de extracción de sulfato no se ve afectado por la presencia de cloruro.
- La presencia de sulfato favorece la extracción de cloruro, ya que los porcentajes de extracción de cloruro son mayores en el sistema ternario (cromo, sulfato, cloruro) que en el sistema binario con cromo y cloruro.
- En el sistema ternario, el porcentaje de extracción de cromo(VI) es independiente de su concentración inicial y tiene valores próximos al 100%. Los porcentajes de extracción de sulfato y cloruro disminuyen respectivamente de 53,7% a 24,4% y de 52,9% a 34,6% cuando la concentración inicial de cromo(VI) aumenta de 1,9 a 29 mol/m³.

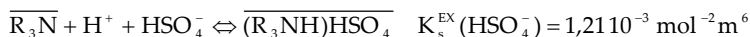
Mecanismo y modelado del equilibrio de extracción

A partir de la información obtenida en la sección anterior, se propuso un mecanismo que permita describir los equilibrios de extracción de las diferentes especies aniónicas, determinando los correspondientes parámetros. Para ello se

analizaron dos sistemas diferentes: i) el sistema binario Alamine336-Sulfato/Cloruro y ii) el sistema ternario (Alamine 336 Cromo/Sulfato/Cloruro), obteniendo las isotermas de equilibrio a temperatura ambiente y en el rango de concentraciones y pH: cromo (9,6-15,4 mol/m³), sulfato (6,8-71 mol/m³), cloruro (4,2-13,5 mol/m³), pH (1-6). De este análisis se obtuvieron los siguientes resultados:

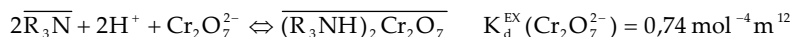
Sistema binario

- La extracción de sulfato y cloruro en un sistema binario se puede describir mediante las siguientes reacciones y parámetros de equilibrio:



Sistema ternario

- La extracción de cromo, sulfato y cloruro en un sistema ternario se puede describir a través de las siguientes reacciones y parámetros de equilibrio:



- Como los valores de los parámetros de equilibrio para la reacción de extracción de sulfato en los sistemas binario ($1,21 \cdot 10^{-3} \text{ mol}^{-2} \text{ m}^6$) y ternario ($1,37 \cdot 10^{-3} \text{ mol}^{-2} \text{ m}^6$) son similares, se pudo concluir que la presencia de cromo no tiene una influencia apreciable sobre la extracción de sulfato en los rangos de concentraciones citados anteriormente.
- El parámetro de equilibrio de la reacción de extracción de cloruro en el sistema ternario (1,52) es mayor que en el sistema binario (0,88). Esta diferencia se atribuye a la participación del cromo en la extracción de

cloruro confirmando la hipótesis de que el mecanismo de extracción de cloruro es diferente dependiendo del sistema analizado.

Análisis de la reacción de reextracción

- La reacción entre el agente reextractante (NaOH) y los complejos organometálicos formados en la etapa de reextracción se consideró instantánea e irreversible debido a que se trabaja con exceso de NaOH.

2. Evaluación Técnica del Proceso de Separación-Concentración (Capítulo 3)

Tras seleccionar la configuración de pertracción en emulsión (EPT) y demostrada su viabilidad para llevar a cabo la separación y concentración de cromo(VI), se procedió a analizar la cinética de las etapas de extracción y reextracción de las diferentes especies aniónicas implicadas en el proceso.

Estudio cinético del proceso de separación-concentración

Los experimentos correspondientes al estudio cinético se llevaron a cabo en un sistema experimental de EPT a escala de laboratorio operando en semi-continuo y con una fase emulsión con una relación de volumen fase orgánica/fase acuosa de reextracción de 4/1. El análisis cinético se llevó cabo mediante dos grupos de experimentos dirigidos a evaluar la influencia de las principales variables de operación: concentración inicial de cromo(VI) en la fase de alimentación y concentración de NaOH en la fase de reextracción.

Influencia de la concentración inicial de cromo(VI) en la fase de alimentación

- El sistema alcanza el régimen pseudo-estacionario rápidamente (<0,2 horas).
- Trabajando en un rango de concentración inicial de cromo(VI) entre 1,9 y 19 mol/m³, los porcentajes de extracción de cromo son superiores al 93% para tiempos de residencia de 1,4 10⁻² h (50 segundos) obteniéndose al final del proceso, valores de concentración en la fase acuosa de reextracción entre 87 y 779 mol/m³ y factores de concentración entre 556 y 5438.

- Cuanto mayor es la concentración inicial de cromo(VI) en la fase acuosa de alimentación menores son los porcentajes de extracción de sulfato y cloruro confirmándose las conclusiones obtenidas en el análisis del equilibrio.
- Las cinéticas de extracción y reextracción de cromo, sulfato y cloruro son independientes de la concentración inicial de cromo(VI) en la fase acuosa de alimentación.

Influencia de la concentración de NaOH en la fase acuosa de reextracción

- Las cinéticas de las etapas de extracción y de reextracción de cromo, sulfato y cloruro son independientes de la concentración del agente reextractante para el rango de concentración de NaOH de 3000-6000 mol/m³.

Modelado matemático del proceso de separación-concentración

Se propuso un modelo para la separación de un sistema multicomponente en régimen difusional y basado en la aproximación de resistencias en serie. Se supone que las reacciones de extracción y reextracción son instantáneas y se consideran tres resistencias al transporte de materia: i) la resistencia en la película difusional de la fase acuosa de alimentación, ii) la resistencia en la membrana y iii) la resistencia en la película difusional de la fase orgánica que rodea los glóbulos de reextracción. De acuerdo al mecanismo de extracción propuesto, el modelado matemático ha sido llevado a cabo teniendo en cuenta las especies aniónicas que participan en las reacciones que constituyen dicho mecanismo, bicromato (HCrO_4^- , i=b), dicromato ($\text{Cr}_2\text{O}_7^{2-}$, i=d), bisulfato (HSO_4^- , i=s) y cloruro (Cl^- , i=c). Las conclusiones obtenidas fueron las siguientes:

- Los equilibrios de las reacciones químicas que tienen lugar en la interfase fase acuosa alimentación-fase orgánica se describieron mediante las expresiones y parámetros obtenidos en el Capítulo 2.
- La Tabla 5.1 muestra los parámetros de transporte característicos del modelo así como su forma de obtención.

- De la comparación de los resultados experimentales y simulados se obtuvieron valores de la desviación estándar para la etapa de extracción comprendidos entre el 0,3% y el 3,4% mientras que para la etapa de reextracción los valores oscilan entre el 5,4% y el 17%. Las desviaciones promedio fueron 2,3% y 8,3% para las etapas de extracción y de reextracción respectivamente.

Tabla 5.1. Valores y forma de obtención de los parámetros de transporte.

Parámetro		Valor	Forma de Obtención
Coeficientes de Transporte de Materia	Película Difusional Fase Líquida (k_{Ll})	$k_{Lb} = k_{Ld}$	Calculado
		k_{Ls}	
		k_{Lc}	
		k_{LH}	
	Membrana (k_{mI})	$k_{mb} = k_{md}$	
		$k_{ms} = k_{mc}$	
	Película Difusional Fase Orgánica (k_o)	$k_o \cdot A_v$	Estimación Paramétrica

- Con los valores de los parámetros mostrados en la Tabla 5.1 se evaluaron las resistencias individuales al transporte de materia llegando a la conclusión de que bajo las condiciones de operación en las que se realizó el estudio, la resistencia al transporte de materia en la película difusional de la fase orgánica para cromo, sulfato y cloruro es despreciable.
- De acuerdo a estos resultados, se simplificó el modelo original obteniendo un modelo de dos resistencias (en la película difusional de la fase acuosa de alimentación y en la membrana) que permitía describir de forma aceptable el

comportamiento cinético del sistema en el intervalo de las condiciones de operación que permite considerar despreciable la acumulación de materia en la fase orgánica. Las desviaciones promedio fueron de 8,6% en la etapa de extracción y 10,6% en la etapa de reextracción, valores superiores a los obtenidos con el modelo de tres resistencias.

Se considera por tanto, que el modelo multicomponente desarrollado y los parámetros característicos del mismo obtenidos en este trabajo (parámetros de equilibrio de las reacciones de extracción y los diferentes coeficientes de transporte de materia, k_L , k_m y K_0) permiten describir de manera satisfactoria las velocidades de las etapas de extracción y reextracción de los diferentes aniones implicados en el proceso de separación y concentración de cromo(VI) cuando se trabaja con la tecnología de emulsión en pertracción en módulos de fibra hueca.

Definición de la selectividad del proceso de separación-concentración

A partir de los valores finales de concentración de cromo, sulfato y cloruro en la fase acuosa de reextracción se definió la selectividad del proceso de separación-concentración:

$$\eta = \left(\frac{[\text{Cr}^{+6}]}{[\text{SO}_4^{2-}] + [\text{Cl}^-]} \right)_{\text{Reextracción}} \quad (5.1)$$

y se propuso una metodología empírica para cuantificar la selectividad del proceso a partir de los valores de las variables de operación dentro del intervalo de condiciones analizadas: $[\text{Cr}]_{\text{inicial}} = 1,9-19 \text{ mol/m}^3$; $\text{pH}_{\text{inicial}} = 1,5-2,1$; $Q^a = 0,005-0,06 \text{ m}^3/\text{h}$ obteniéndose las siguientes conclusiones:

- La selectividad aumenta exponencialmente desde 0,062 a 2,3 cuando la concentración inicial de cromo(VI) en la fase acuosa de alimentación aumenta desde 1,9 y 19 mol/m³.
- Al aumentar el pH inicial (dentro del intervalo 1,5-2,1) y el caudal de la fase acuosa de alimentación (dentro del intervalo 0,005-0,06 m³/h), aumenta la selectividad del proceso de separación-concentración dentro en el intervalo 0,3-160.

3. Diseño Óptimo del Proceso de Separación-Concentración (Capítulo 4)

Finalmente, se desarrolló una metodología basada en técnicas de optimización matemática, para llevar a cabo el diseño óptimo de una red de tratamiento de corrientes con contaminantes metálicos mediante la tecnología de pertracción en emulsión. Partiendo de una representación de alternativas mediante superestructuras, se procedió al modelado matemático de las mismas desarrollando a continuación, la estrategia de solución que permite resolver los problemas generados con el fin de obtener la configuración óptima de proceso que permite alcanzar, con el mínimo coste, los objetivos planteados: i) reducir la concentración del contaminante por debajo del valor límite requerido y ii) concentrarlo selectivamente hasta el nivel deseado según cual sea su destino final.

Las superestructuras se modelaron inicialmente de forma rigurosa (problema P1) obteniendo posteriormente un modelo simplificado (P2). El modelo riguroso se resolvió mediante técnicas de optimización local (solver comercial CONOPT 3.0 de GAMS) empleando como punto inicial la solución del modelo simplificado obtenida mediante técnicas de optimización global (solver comercial BARON 7.2.5). Para resolver aquellos problemas altamente no lineales que no pueden ser resueltos con el solver comercial BARON 7.2.5 se desarrolló un algoritmo basado en técnicas de descomposición lagrangiana.

Con el fin de determinar el número óptimo de módulos de fibras huecas, el problema se resolvió para superestructuras con 2, 3 y 4 módulos de tratamiento obteniéndose las siguientes conclusiones:

- Para el caso de dos módulos, no se obtuvieron soluciones factibles de los problemas P1 y P2.
- Para tres y cuatro módulos, el algoritmo de descomposición lagrangiana requiere tiempos de CPU inferiores al solver comercial BARON a la hora de resolver los respectivos problemas P2. Para el caso de tres módulos, el tiempo se reduce de 20,81 a 2,08 segundos. Cuando se emplean cuatro módulos, BARON necesita más de 10 horas para obtener la solución

mientras que con el algoritmo el problema es resuelto en 611,07 segundos. Por tanto, el algoritmo de descomposición lagrangiana propuesto permite disminuir el tiempo de solución con respecto al requerido por el solver comercial BARON 7.2.5,

- Se concluye que la configuración óptima que permite alcanzar los objetivos de tratamiento y concentración contiene 3 módulos de tratamiento dispuestos en serie-paralelo y con un área total de membrana de 591 m². Las Figuras 5.1 y 5.2 muestran las configuraciones óptimas para la fase acuosa de alimentación y para la fase emulsión.

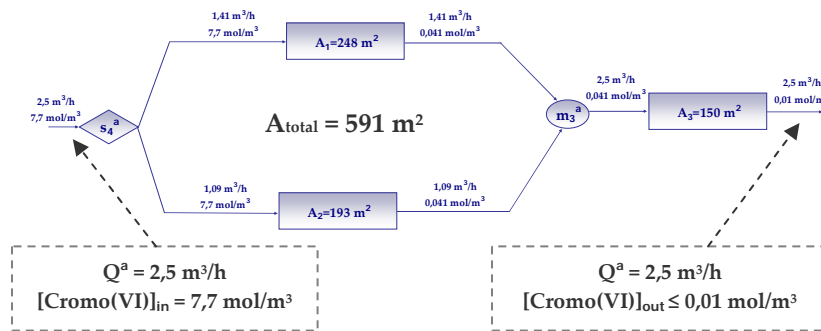


Figura 5.1. Configuración óptima para la fase acuosa de alimentación.

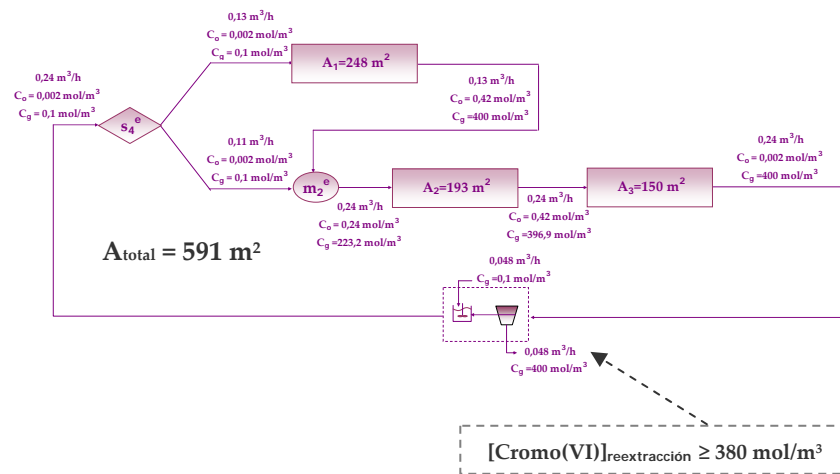


Figura 5.2. Configuración óptima para la fase emulsión.

5. FINAL CONCLUSIONS

This Thesis aims at the development of the methodology for the optimal design of selective liquid membrane processes, innovative alternatives, for the separation and selective recovery of raw materials and valuable compounds from multicomponent systems. The developed methodology has been applied to the remediation of polluted groundwater containing hexavalent chromium as a consequence of effluent leaking from surface deposition of industrial wastes. Furthermore, other competitive anionic species (mainly sulphate and chloride anions) were also present in groundwaters due to the specific location being close to the shore. The study has been carried out working with the emulsion pertraction technology (EPT) using hollow fiber contactors; this is considered a novel alternative able to overcome the limitations associated to other membrane-based solvent extraction technologies.

The proposed methodology begins with the analysis and characterisation of the extraction and back-extraction system followed by the kinetic study and mathematical modeling of the separation-concentration process. Finally, a novel design methodology based on the application of mathematical optimization techniques has been developed in order to determine the optimal process configuration able to achieve, at minimum cost, the separation and concentration objectives.

The main conclusions achieved from the analysis of the results obtained in the Thesis are the following:

1. Characterisation and Analysis of the Extraction and Back-Extraction System (Chapter 2)

Effluent characterisation

- In order to avoid calcium precipitation inside the membrane contactors, the study was carried out working with acidic solutions that contained the main anionic compounds present in the groundwaters: chromium(VI), 9.6-26 mol/m³; sulphate, 10-29 mol/m³; chloride, 10-33 mol/m³.

Selection of the extraction and back-extraction agents

- From the literature, Alamine 336 (tertiary amine) and NaOH were selected respectively as extraction and back-extraction agents suitable for the selective separation and concentration of chromium(VI) at acidic pH.

Analysis of the competitive species co-extraction

In order to analyse the co-extraction of competitive species (sulphate and chloride), several experiments were performed in a rotary equipment varying the initial chromium concentration and working with three different systems: i) a binary system with chromium and sulphate anions, ii) a binary system with chromium and chloride anions and, iii) a tertiary system with chromium, sulphate and chloride anions. The main conclusions were,

- The influence of sulphate and chloride anions on the extraction of chromium can be considered negligible.
- The sulphate extraction percentage is not affected by the presence of chloride anions in the aqueous feed solution.
- The chloride extraction percentages obtained in the tertiary system (chromium, sulphate and chloride), are higher than the values reached in the binary system with chromium and chloride. Therefore, the presence of sulphate anions improves the extraction of chloride.
- In the tertiary system, the influence of the initial chromium concentration on the chromium extraction percentage (close to 100%) can be considered negligible. However, increasing the initial chromium(VI) concentration from 1.9 to 29 mol/m³, the sulphate and chloride extraction percentages decrease respectively, from 53.7% to 24.4% and from 52.9% to 34.6%.

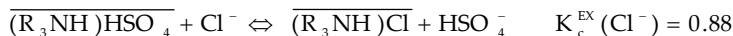
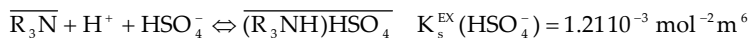
Analysis and mathematical modeling of the extraction equilibria

From the analysis of the information obtained above, a reaction mechanism able to describe the extraction equilibria of the anionic species was proposed. In order to determine the equilibria parameters of the extraction reactions, two different

systems were analyzed: i) the binary system Alamine 336-Sulphate/Chloride and, ii) the tertiary system Alamine 336-Chromium/Sulphate/Chloride. The equilibria isotherms for all the species (at a 298) were experimentally obtained in both systems working with aqueous feed solutions containing different concentrations of chromium (9.6-15.4 mol/m³), sulphate (6.8-71 mol/m³) and chloride (4.2-13.5 mol/m³) an in the pH range 1-6. From this analysis different results were obtained:

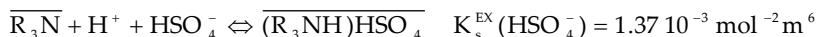
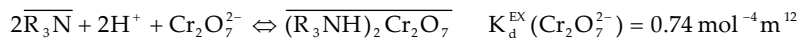
Binary System

- The extraction of sulphate and chloride anions in a binary system can be described by the following reactions and equilibria parameters:



Tertiary system

- The extraction of chromium, sulphate and chloride anions in a tertiary system can be described by the following reactions and equilibria parameters:



- Comparing the values of the equilibrium parameters for sulphate anions in both systems, binary ($1.21 \cdot 10^{-3} \text{ mol}^{-2} \text{ m}^6$) and tertiary ($1.37 \cdot 10^{-3} \text{ mol}^{-2} \text{ m}^6$), it can be concluded that there is no significant difference between them and consequently, the influence of chromium anions in the extraction of sulphate can be considered negligible under the concentration ranges previously specified.

- After comparison of the values of the extraction parameters of chloride, 0.88 (binary system) and 1.52 (tertiary system) it can be concluded that the presence of chromium species exerts influence in the extraction of chloride anions concluding, that the extraction mechanism for chloride anions changes depending on the system under study.

Analysis of the back-extraction reaction

- The reaction between the stripping agent (NaOH) and the organometallic complexes formed in the extraction step can be considered totally shifted to the right due to the high concentration of NaOH.

2. Technical Evaluation of the Separation-Concentration Process (Chapter 3)

After having selected the emulsion pertraction technology (EPT) and demonstrated the viability of the separation and concentration of chromium(VI), the kinetic analysis of the extraction and back-extraction steps was performed.

Kinetic study of the separation-concentration process

The kinetic experiments were carried out in a laboratory EPT experimental set-up operating in semi-continuous mode. The emulsion phase was prepared by dispersion of the stripping solution into the organic phase being the volume ratio 1/4. The kinetic analysis was performed by means of two different groups of experiments in order to evaluate the influence of the main operation variables: initial chromium(VI) concentration in the aqueous phase solution and NaOH concentration in the back-extraction solution.

Influence of the initial chromium(VI) concentration in the aqueous feed solution

- The pseudo steady state of the system is reached rapidly (<0.2 h).
- Working in the range of chromium(VI) concentration between 1.9 and 19 mol/m³, the extraction percentages of chromium are higher than 93% for a residence time of 1.4 10² h (50 seconds). On the other hand, the chromium concentration in the stripping phase at the end of the process reaches values

between 87 y 779 mol/m³, thus concentration factors between 556 and 5438 are reached before depletion of the stripping reagent.

- The higher initial chromium(VI) concentration is, the lower sulphate and chloride extraction percentages are. This fact confirms the conclusions obtained from the equilibrium analysis.
- The extraction and back-extraction kinetics of chromium, sulphate and chloride anions are independent of the initial chromium(VI) concentration in the aqueous feed solution.

Influence of the NaOH concentration in the stripping solution

- In the studied range of variables, 3000 mol/m³ ≤ NaOH ≤ 6000 mol/m³, and working with excess of OH⁻ ions there is no influence of the NaOH concentration in the extraction and back-extraction kinetics of chomium(VI), sulphate and chloride anions.

Mathematical modeling of the separation-concentration process

A diffusional multicomponent separation mathematical model of the EPT process based on the in-series resistance approach was proposed. The extraction and back-extraction reactions are assumed to take place instantaneously and three different mass transport resistances were taken into account: i) mass transport resistance in the aqueous phase stagnant layer, ii) mass transport resistance through the membrane and, iii) mass transport resistance in the organic phase stagnant layer that surrounded the emulsion droplets. In agreement with the extraction mechanism proposed, the mathematical modeling took into account all the anionic species that participate in the separation process, bichromate ($HCrO_4^-$, i=b), dichromate ($Cr_2O_7^{2-}$, i=d), bisulphate (HSO_4^- , i=s) and chloride (Cl^- , i=c). The conclusions obtained are as follows:

- The equilibria of the extraction reactions that take place in the interface between the aqueous feed solution and the organic phase were described by means of the equations and parameters obtained in Chapter 2.

- Table 5.1 shows the model mass transport parameters and the way in which they have been obtained.
- From the comparison of experimental and simulated data, the following ranges of values of the standard deviation were obtained: 0.3%-3.4% for the extraction step and 5.4-17% for the back-extraction step, being the average values 2.3% and 8.3% respectively.

Table 5.1. Mass Transport Coefficients.

Parameter		Value	Obtention
Mass Transport Coefficients	Aqueous Phase Stagnant Layer (k_{Ll})	$k_{Lb} = k_{Ld}$	Calculated
		k_{Ls}	
		k_{Lc}	
		k_{LH}	
	Membrane (k_{mi})	$k_{mb} = k_{md}$	
		$k_{ms} = k_{mc}$	
	Organic Phase Stagnant Layer (k_o)	$k_o \cdot A_v$	Paremetric Estimation

- Making use of the values of the mass transport coefficients shown in Table 5.1, the individual mass transfer resistances were evaluated concluding that under the experimental conditions, the kinetic control is shared between the feed and the membrane mass transport phenomena while the resistance associated to the organic phase contained in the emulsion globules can be considered negligible.
- Then, the mathematical model was simplified accounting for two resistances (in the aqueous phase stagnant layer and in the membrane) able to describe

the kinetic behaviour of the system under the operating conditions; mass accumulation in the organic phase was neglected. The average standard deviations obtained with this model for the extraction and back-extraction steps were respectively 8.6% and 10.6%.

As a final conclusion, it can be said that the proposed multicomponent model with the characteristic parameters (equilibria parameters of the extraction reactions and mass transport coefficients, k_L , k_m y K_0) describes satisfactorily the kinetics of the extraction and back-extraction steps of the different anionic compounds that participate in the selective separation and concentration of chromium(VI) by means of the emulsion pertraction technology in hollow fiber contactors.

Selectivity of the separation-concentration process

The selectivity of the separation-concentration process was defined as a function of the final chromium, sulphate and chloride concentrations in the back-extraction solution as follows:

$$\eta = \left(\frac{[\text{Cr}^{+6}]}{[\text{SO}_4^{2-}] + [\text{Cl}^-]} \right)_{\text{Back-Extraction}} \quad (5.1)$$

An empirical methodology was proposed in order to make possible the quantitative evaluation of the process selectivity as a function of the following operating variables: $[\text{Cr}]_{\text{initial}} = 1.9-19 \text{ mol/m}^3$; $\text{pH}_{\text{initial}} = 1.5-2.1$; $Q^a = 0.005-0.06 \text{ m}^3/\text{h}$ (aqueous phase flowrate). From this analysis the following conclusions were obtained:

- The selectivity increases exponentially from 0.062 to 2.3 when the initial chormium(VI) concentration in the aqueous feed solution increases from 1.9 y 19 mol/m³.
- The higher initial pH (within the range 1.5-2.1) and the higher aqueous feed phase flowrate (within the range 0,005-0,06 m³/h) are, the higher process selectivity is (within the range 0.3-160).

3. Optimal Process Design of the Separation-Concentration Process (Chapter 4)

Finally, a novel design methodology based on the application of mathematical optimization techniques has been developed in order to determine the optimal EPT process configuration able to achieve, at minimum cost, the separation and concentration objectives, i) the contaminant removal up to the required concentration level and, ii) the selective contaminant recovery to obtain a concentrated solution that can be reused elsewhere. The different design alternatives were represented by means of network superstructures that were modeled generating optimization problems that were solved following the solution strategy developed in this study.

The network superstructures were initially modeled rigorously (problem P1) and making several simplifications (problem P2). The rigorous model was solved by local optimization techniques (commercial solver GAMS/CONOP 3.0) using as initial point the global optimal solution of the simplified model. Two different global optimization techniques were employed: the commercial solver GAMS/BARON 7.2.5 for small problems and a Lagrangean Decomposition Algorithm (LDA) for highly non-linear problems.

In order to determine the optimal number of hollow fiber modules, the problem was solved for network superstructures with 2, 3 and 4 treatment modules obtaining the following conclusions:

- For network superstructures with 2 modules, no feasible solutions were obtained.
- For network superstructures with 3 membrane modules the simplified model (P2) was solved with both GAMS/BARON7.2.5 and LDA being the CPU times 20.81 and 2.08 seconds, respectively. For network superstructures with 4 membrane modules it was not possible to solve the simplified model (P2) in less than 10 hours, however with the LDA the problem P2 was solved in 611.07 seconds. Therefore, the Lagrangean Decomposition Algorithm developed in this work reduces the CPU time

required by GAMS/BARON 7.2.5 to solve the simplified model (P2) to global optimality.

- It can be concluded that a network configuration with 3 treatment modules combined in series and parallel was the most suitable process configuration to comply, at minimum cost, with the concentration specifications in the outlet streams. Figures 5.1 y 5.2 shows the optimal process configurations for the aqueous feed solution and the emulsion phase.

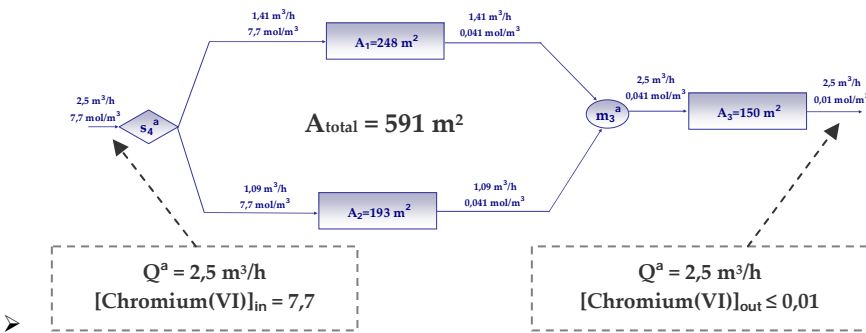


Figure 5.1. Optimal Process Configuration for the Aqueous Feed Solution.

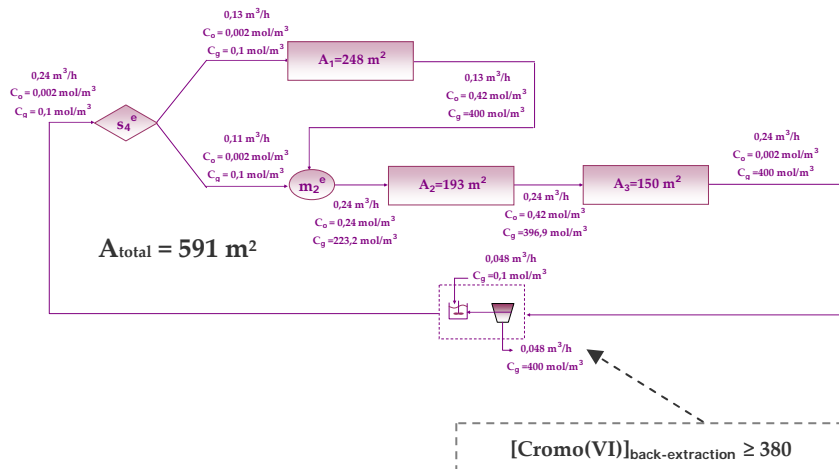


Figure 5.2. Optimal Process Configuration for the Emulsion Phase.

A1. Difusión de Resultados

I) Artículos en Revistas Internacionales:

- **Bringas, E., San Román, M.F., Urtiaga, A.M., Ortiz, I. (2008), "Membrane Contactors (NDSX and EPT Technologies): An Innovative Alternative for the Remediation of Effluents Containing Metallic Pollutants", *Int. J. Environment and Waste Management*, Aceptado y en prensa.**
- **Bringas, E., Karupiah, R., San Román, M.F., Ortiz, I., Grossmann, I.E. (2007), "Optimal Groundwater Remediation Network Design using Selective Membranes", *Ind. Eng. Chem. Res.*, 46, 5555-5569.**
- **San Román, M.F., Bringas, E., Ortiz, I., Grossmann, I.E. (2007), "Optimal Synthesis of an Emulsion Pertraction Process for the Removal of Pollutant Anions in Industrial Wastewater Systems", *Comp. Chem. Eng.*, 31, 456-465.**
- **Bringas, E., San Román, M.F., Ortiz, I. (2006), "Separation and Recovery of Anionic Pollutants by the Emulsion Pertraction Technology. Remediation of Polluted Groundwaters with Cr(VI)", *Ind. Eng. Chem. Res.*, 45, 4295-4303.**
- **Bringas, E., San Román, M.F., Ortiz, I. (2006), "Removal of Anionic Pollutants from Groundwaters using Alamine 336: Chemical Equilibrium Modelling", *J. Chem. Technol. Biot.*, 81, 1829-1835.**
- **Bringas, E., San Román, M.F., Urtiaga, A.M., Ortiz, I. (2006), "Intensification of Membrane Processes. Remediation of Groundwaters by Emulsion Pertraction as a Case Study", *Desalination*, 200, 459-461.**
- **Ortiz, I., Bringas, E., Samaniego, H., San Román, M.F., Urtiaga, A.M., (2006), "Membrane Processes for the Efficient Recovery of Anionic Pollutants", *Desalination*, 193, 375-380.**

II) Comunicaciones a Congresos Internacionales:

- **Bringas, E., San Román, M.F., Ortiz, I. (2008)**, "Converting Membrane-Based Solvent Extraction Networks into Sustainable Processes. Remediation of Groundwaters Polluted with Cr(VI) as Case Study". *International Solvent Extraction Conference (ISEC2008)*, Tucson, Arizona (USA), 15-19 Septiembre, 2008. Aceptado.
- **Bringas, E., Criscuoli, A., San Román, M.F., Ortiz, I., Drioli, E. (2007)**, "Membrane-Based Oxidation Processes for the Remediation of Polluted Groundwaters with As(III)", *6th European Congress of Chemical Engineering (ECCE -6)*, Copenague (Dinamarca), 16-20 Septiembre, 2007. Póster.
- **San Román, M.F., Bringas, E., Carrera, J.A., Ortiz, I. (2007)**, "Emulsion Pertraction Technology in Hollow Fiber Modules: Application to Metallic Valorisation from Wastewater", *8th International Conference on Chemical & Process Engineering (ICheAP-8)*, Ischia (Italia), 24-27 Junio, 2007. Comunicación Oral.
- **Bringas, E., San Román, M.F., Ortiz, I. (2007)**, "Optimal Design of Sustainable Technologies for the Remediation of Polluted Groundwaters", *1st International Congress on Green Process Engineering (GPE 2007)*, Toulouse (Francia), 24-26 Abril, 2007. Póster.
- **Bringas, E., San Román, M.F., Urtiaga, A.M., Ortiz, I. (2006)**, "Intensification of Membrane Processes. Remediation of Groundwaters by Emulsion Pertraction as a Case Study", *Euromembrane 2006*, Taormina (Italia), 21-28 Septiembre, 2006. Comunicación Oral.
- **Bringas, E., (2006)**, "Optimal Process Design for Selective Recovery of Anionic Pollutants", *8th Network Young Membrains (NYM 8)*, Rende (Italia), 21-23 Septiembre 2006. Comunicación Oral.
- **Ortiz, I., Bringas, E., Samaniego, H., San Román, M.F., Urtiaga, A.M., (2006)**, "Membrane Processes for the Efficient Recovery of Anionic Pollutants", *International Congress on Membranes and Membrane Processes (ICOM 2005)*, Seul (Corea), 21-26 Agosto, 2005. Comunicación Oral.

- **Bringas, E., Samaniego, H., San Román, M.F., Ortiz, I (2005)**, "Clean Technologies in the Treatment of Waste Effluents. Recovery of Metallic Pollutants", *7th World Congress of Chemical Engineering (WCCE 7)*, Glasgow (Escocia), 10-14 Julio, 2005. Póster.
- **San Román, M.F., Bringas, E., Ortiz, I., Grossmann, I.E. (2005)**, "Optimal Synthesis of an Emulsion Pertraction Process for the Removal of Pollutant Anions in Industrial Wastewater Systems", *European Symposium on Computer Aided Process Engineering (ESCAPE15)*, Barcelona (España), 29 Mayo-1 Junio, 2005. Comunicación Oral .
- **Bringas, E. (2004)**, "Purification of Polluted Groundwater using Emulsion Pertraction Technology. Chromium(VI) Removal", *6th Network Young Membrains (NYM 6)*, Hamburgo (Alemania), 22-24 Septiembre 2004. Comunicación Oral.

A2. Modeling of Membrane Oxidation Processes

En este anexo se recogen el informe correspondiente al trabajo realizado durante la estancia en en *L'Istituto per la Tecnologia delle Membrane* (Rende, Italia) bajo la supervisión del Prof. Enrico Drioli. Este trabajo ha dado lugar a una contribución en el “6th European Congress of Chemical Engineering (ECCE-6)”, celebrado en Copenague (Dinamarca) entre el 16 y el 20 Septiembre de 2007.

Introduction

The presence or arsenic in the groundwater reservoirs of some countries like India and Bangladesh is an environmental problem of concern. It is generally caused by the filtration of polluted water produced by dissolution of natural arsenic initially contained in minerals and sediments.¹ In the case of surface water pollution, arsenic is mainly present as As⁺⁵ while in groundwater this pollutant is mainly present as As⁺³ due to the absence of oxygen.²

Different technologies can be used in the treatment of groundwater containing arsenic but membrane technologies can be considered as a promising alternative to reduce the level of metallic pollutants in groundwater.^{3,4,5} In particular, reverse osmosis and nanofiltration are proven technologies to achieve this particular purpose.^{6,7,8,9}

To improve the efficiency of membrane technologies it is necessary to oxidize As⁺³ to As⁺⁵ because the rejection percentage is higher for the oxidized species.⁸

The arsenic oxidation has been traditionally performed using different oxidizing agents (ozone, chlorine, hydrogen peroxide, manganese oxides, etc.) and different contact equipments (spray towers, packed columns, etc.).^{8,10,11,12}

This work proposes a pre-treatment step for oxidizing arsenic with a gaseous oxidant using membrane contactors. In particular, it is focused on the modeling of the As⁺³ oxidation with ozone using hollow fiber contactors as reactors.

The developed model can be also applied to other oxidation reactions, as, for example, the oxidation of organic pollutants contained in water.

Work carried out

State of the Art.

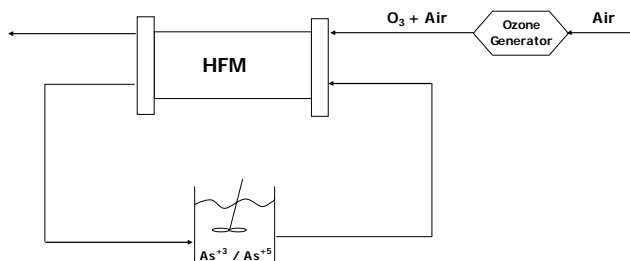
The objective of this task is to have an idea about the “state of the art” concerning to arsenic oxidation. The literature shows different works related to the arsenic oxidation using different oxidizing agents. Table 1 reports the main advantages and disadvantages of the different agents used for oxidizing arsenites to arsenates.

System Definition.

After reviewing the literature, the definition of the system was performed. In particular, the oxidation is performed using ozone as oxidant and a hollow fiber membrane contactor as membrane reactor. Figure 1 shows the process setup considered for the modeling. The liquid stream is re-circulated at the shell side of the module while the gaseous feed is sent to the fibers lumen. An efficiency of 60 % has been considered for the ozone generator.

Table 1. Advantages and disadvantages of agents used for oxidation of As^{+3} to As^{+5} ¹³

Agent	Advantages	Disadvantages
Air/O ₂	Oxidation agent is readily available everywhere in the world and is not hazardous	Oxidation is slow and additional equipment to speed it up increases system capital and operating costs
O ₃	Oxidation agent is generated at point of use which reduces exposure to ozone	Ozone is a known health hazard and the oxidation system has high operating and maintenance costs
H ₂ O ₂	The oxidation agent is a safe solution that can be manually or automatically metered in	The oxidation reaction may be too slow for practical use and oxidant solution can lose oxidation power
Liquid Cl ₂	The oxidation reaction is very fast and completely removes any potential disease carriers	The oxidant is difficult to store or transport safely and system parts can be degraded by corrosion
ClO ⁻	The oxidation reaction is relatively fast and removes any potential disease carriers	The system parts can be degraded by corrosion and oxidant solution can lose oxidation power with time
MnO ₄ ⁻	The oxidation agent is a safe solution that can be manually or automatically metered in	The oxidation reaction results in a solid manganese compound that may interfere with system operation
Fe ⁺³ or Mn ⁺⁴	The system design allows oxidation and filtration steps to be combined in one unit	Iron (III) compounds can hydrolyze to form gelatinous solids which may plug up the oxidation/filtration bed
Fenton's Reagent	The oxidation rate is faster than hydrogen peroxide and oxidant solution more stable	Operator error in mixing the iron (II) compound with the hydrogen peroxide can degrade the results

**Figure 1.** Process setup

The hollow fiber module used in the process simulation is a Liqui-Cel® Extra-Flow 2.5 × 8 contactor with fibers X50. The main characteristics of this module are shown in Table 2.¹⁴

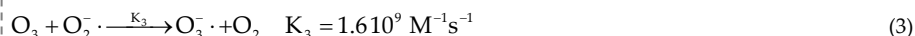
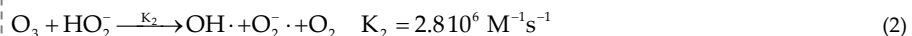
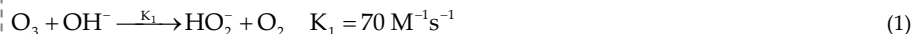
Table 2. Characteristics of the hollow fiber contactor

Provider:	Celgard
Contactor type:	Liqui-Cel extra-flow 2.5 in. × 8 in. (64 mm × 203 mm)
Shell diameter	$d_S = 6.3 \text{ cm}$
Fiber bundle diameter	$d_a = 4.7 \text{ cm}$
Distribution tube diameter	$d_i = 2.2 \text{ cm}$
Overall contact area (based on outer fiber diameter)	$A_S = 1.4 \text{ m}^2$
Overall contact area (based on inner fiber diameter)	$A_F = 1.13 \text{ m}^2$
Fiber material/type	Polypropylene
Number of fibers	9,950
Outer fiber diameter	$d_o = 300 \mu\text{m}$
Inner fiber diameter	$d_F = 240 \mu\text{m}$
Fiber wall thickness	$e = 30 \mu\text{m}$
Fiber porosity	$\epsilon = 0.4$
Pore tortuosity	$\tau = 2.25$
Pore diameter	$0.03 \mu\text{m}$

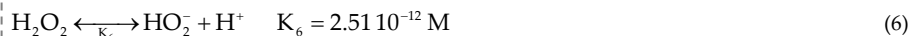
Kinetic Data.

The next step was the search of kinetic data for the oxidation reaction between arsenite (H_2AsO_3^-) and ozone. This reaction is described by a second – order kinetics being the value of the kinetic constant $7 \text{ M}^{-1} \text{ s}^{-1}$.^{15,16} As consequence of the low value of this constant the direct oxidation of arsenic with ozone is too slow.

Otherwise, if the reaction between ozone and the solute is not fast, the ozone decomposition takes place due to its unstable behaviour in aqueous solutions. The major secondary oxidant formed from ozone decomposition in water is the OH radical. The ozone decomposition involves the following reactions:^{15,16,17,18,19}



$pH < 8^*$



(*) In this work, it was assumed that solutions have a $pH < 8$

The oxidation reaction between arsenite and hydroxide radicals can be described by a second-order kinetics being the value of the kinetic constant $K_{\text{ox}} = 8.5 \cdot 10^9 \text{ M}^{-1} \text{ s}^{-1}$.¹⁵

As was shown in reactions (1) and (2), the initiation of ozone decomposition can be carried out by OH^- or HO_2^- . In absence of hydrogen peroxide, the ozone decomposition is initiated by its reaction with OH^- . The value of the kinetic constant of reaction (1) is low and consequently the initiation rate is slow. In order to increase the initiation rate it is possible to add H_2O_2 , so that

reaction (2) can occur. Being the kinetic constant of this reaction 4 10⁴ times greater than the one for reaction (1), the OH radical production is enhanced.¹⁸

Model proposal.

At this point, the different mass transfer steps were proposed. Figure 2 shows a fiber cross section with the mass transport hypothesis taken into account to develop the mathematical model.

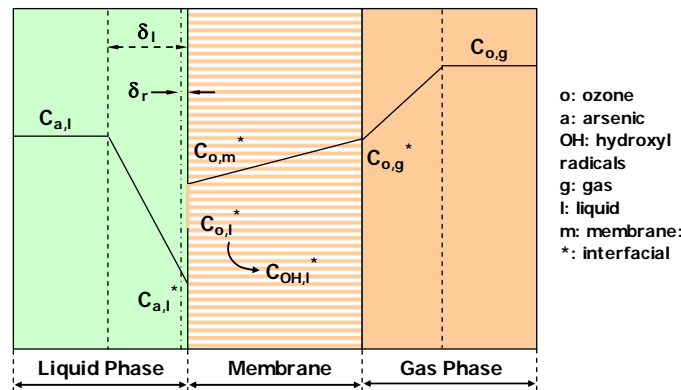


Figure 2. Mass transport hypothesis

In this case several hypotheses have been taken into account:

- The membrane is considered completely hydrophobic and consequently the pores are filled exclusively by gas.
- The dissolution of ozone in the liquid phase is described by the Henry's law.
- The arsenic and ozone that reach the interface react (equality between fluxes and reaction rates).
- The oxidation reaction takes place in an infinitesimal liquid volume close to the membrane.
- Pseudo - steady state.
- The radicals produced as consequence of the ozone decomposition remain behind the infinitesimal liquid volume close to the membrane.

The mass transport fluxes corresponding to the mass transport steps showed in Figure 2 can be described by the following equations:

$$J_{a,l} = K_L \cdot (C_{a,l} - C_{a,l}^*) \quad (7)$$

$$J_{o,g} = K_g \cdot (C_{o,g} - C_{o,g}^*) \quad (8)$$

$$J_{o,m} = K_m \cdot (C_{o,m}^* - C_{o,m}^*) \quad (9)$$

where K_L , K_g and K_m are respectively the mass transport coefficients of the corresponding solutes in the aqueous phase stagnant layer, the gaseous phase stagnant layer and the membrane.

The mass transport coefficient of arsenite compounds in the aqueous phase stagnant layer (K_L) was calculated according to the following expression:

If $Re \geq 1.65$ then²⁰

$$K_L = \frac{D_a}{(2 \cdot r_o)} 0.9 \cdot e^{[0.4 \ln(Re)]} e^{[0.33 \ln(Sc)]} \quad (10)$$

If $Re < 1.65$ then²¹

$$K_L = \frac{D_a}{(2 \cdot r_o)} 0.435 \cdot e^{[1.2 \ln(Re)]} e^{[0.33 \ln(Sc)]} \quad (11)$$

where D_a is the diffusivity of arsenite in water ($3.2 \cdot 10^{-9} \text{ m}^2/\text{s}$);²² r_o is the outer diameter of the fiber (m); Re and Sc are the Reynolds and Schmidt dimensionless numbers.

The mass transport coefficient of ozone in the membrane was calculated with the following correlation:²³

$$K_M = \frac{D_o \cdot \varepsilon_M}{0.5 \cdot (d_o - d_f) \cdot \tau_M} \quad (12)$$

$$\frac{1}{D_o} = \frac{1}{D_{k,o}} + \frac{1}{D_{m,o}} \quad (13)$$

$$D_{k,o} = \frac{1}{3} \frac{\varepsilon_M \cdot d_0}{\tau_M} \sqrt{\frac{8 \cdot R \cdot T_g}{\pi \cdot M}} \quad (14)$$

where D_o is the effective diffusion coefficient of ozone through the membrane (m^2/s); $D_{k,o}$ is the Knudsen diffusion coefficient of ozone (m^2/s); $D_{m,o}$ is the continuous diffusion coefficient of ozone in air ($1.3 \cdot 10^{-5} \text{ m}^2/\text{s}$); d_o and d_f are, respectively, the outer and inner diameters of the fiber (m); ε_M is the porosity of the membrane and τ_M is the pore tortuosity; R is the universal gases constant (J/mol K); T_g is the gas temperature (K) and M is the molecular weight of the solute (Kg/mol).

Finally, the mass transport coefficient of ozone in the gaseous phase stagnant layer was calculated with the Lévêque's equation:²⁴

$$\frac{K_g \cdot d_f}{D_{o,m}} = 1.62 \left(\frac{d_f^2 \cdot u}{L \cdot D_{o,m}} \right)^{1/3}$$

(15)

where u is the fluid velocity in the fiber (m/s) and L is the effective length of the fiber (m).

The ozone concentrations in the gaseous and liquid phases are related by the Henry's dimensionless coefficient:²³

$$H_o^* = \frac{5.6 \cdot 10^{-4} \cdot H_o}{R \cdot T_g} = \frac{C_{o,m}^*}{C_{o,l}^*} \quad (16)$$

$$H_o = 3.89 \cdot 10^{12} \cdot [\text{OH}]^{0.035} \cdot \exp\left(-\frac{2428}{T_l}\right) \quad (17)$$

where H_o^* is the dimensionless Henry's coefficient; H_o is the Henry's coefficient for the system ozone / water (Kpa/molfr); $[OH]$ is the hydroxyl anions concentration in the aqueous phase (mol/L) and T_l is the liquid temperature (K).

Apart from the mass transport equations, the model also includes the mass balances of arsenic and ozone both in the module and the tank. The module mass balances of arsenic in the aqueous feed solution can be expressed by the following partial differential equation:

$$\begin{aligned} A_1 \frac{\partial C_{a,l}}{\partial t} + F_l \frac{\partial C_{a,l}}{\partial z} &= -\pi \cdot n_F \cdot \delta_r \cdot (d_F + \delta_r) \cdot r_{ox} \\ A_1 = \frac{\pi}{4} (d_{shell}^2 - n_F \cdot d_F^2) \\ z = 0 \Rightarrow C_{a,l} &= C_{a,T} \\ t = 0 \Rightarrow C_{a,l} &= C_{a,l}(t = 0) \end{aligned} \quad (18)$$

The module mass balance of ozone in the gas phase is described by the following equation:

$$\begin{aligned} A_g \frac{\partial C_{o,g}}{\partial t} + F_g \frac{\partial C_{o,g}}{\partial z} &= -\pi \cdot n_F \cdot \delta_r \cdot (d_F + \delta_r) \cdot r_{dec} \\ A_g = \frac{\pi}{4} d_o^2 \cdot n_F \\ z = 0 \Rightarrow C_{o,g} &= C_{o,g}^{in} \\ t = 0 \Rightarrow C_{o,g} &= C_{o,g}(t = 0) \end{aligned} \quad (19)$$

The module mass balance of hydroxyl radicals present in the aqueous phase as consequence of ozone decomposition can be described by the following equation:

$$\begin{aligned} A_1 \frac{\partial C_{OHrad,l}^*}{\partial t} + F_l \frac{\partial C_{OHrad,l}^*}{\partial z} &= \pi \cdot n_F \cdot \delta_r \cdot (d_F + \delta_r) \cdot r_{OHrad} \\ z = 0 \Rightarrow C_{OHrad,l}^* &= 0 \\ t = 0 \Rightarrow C_{OHrad,l}^* &= 0 \end{aligned} \quad (20)$$

where A_1 and A_g are respectively the cross sections of the shell side and the fibers in the module (m^2); n_F is the number of hollow fibers; δ_r is the infinitesimal thickness of the layer where the oxidation reaction takes place (m). It is considered as fraction of the thickness of the aqueous phase stagnant layer (δ_l); F_a and F_g are respectively the flowrates of the aqueous and liquid phases; z is the axial dimension (m); t is the time (s) and r is the reaction rate ($mol/m^3 s$). If steady state is assumed the accumulation term can be considered negligible.

The value of the δ_r can be calculated as a function of δ_l with the following equations:

$$\delta_r = \frac{D_a}{K_L} \quad (21)$$

$$\delta_r = \alpha \cdot \delta_l \Rightarrow 0 < \alpha < 1 \quad (22)$$

being α a parameter that represents the fraction of the liquid phase stagnant layer where the oxidation reaction is taking place.

The oxidation reaction between arsenic and hydroxyl radicals has been described by a second order kinetic expression:

$$r_{\text{ox}} = K_{\text{ox}} \cdot C_{\text{a},l}^* \cdot C_{\text{OH},l}^* \quad (23)$$

where K_{ox} is the kinetic parameter of the oxidation reaction ($\text{m}^3/\text{mol s}$).

The kinetic expression for ozone decomposition can be derived from reactions (1)-(3):

$$r_{\text{dec}} = K_1 \cdot C_{\text{o},l}^* \cdot C_{\text{OH}^-,l}^* + K_2 \cdot C_{\text{o},l}^* \cdot C_{\text{HO}_2^-,l}^* + K_3 \cdot C_{\text{o},l}^* \cdot C_{\text{O}_2^-,l}^* \quad (24)$$

The kinetic expression for hydroxyl radicals can be expressed as the difference between the radicals produced by ozone decomposition and the radicals consumed in the arsenic oxidation:

$$r_{\text{OHrad}} = K_2 \cdot C_{\text{o},l}^* \cdot C_{\text{HO}_2^-,l}^* + K_5 \cdot C_{\text{HO}_3^-,l}^* - K_{\text{ox}} \cdot C_{\text{a},l}^* \cdot C_{\text{OH},l}^* \quad (25)$$

The module mass balances for the different intermediates that are involved in the ozone decomposition should also be taken into account:

$$\begin{aligned} A_l \frac{\partial C_i^*}{\partial t} + F_l \frac{\partial C_i^*}{\partial z} &= \pi \cdot n_F \cdot \delta_r \cdot (d_F + \delta_r) \cdot r_i \\ z = 0 \Rightarrow C_i &= C_i^{\text{in}} \\ t = 0 \Rightarrow C_i &= C_i(t=0) \\ i &= \text{HO}_2^-; \text{OH}^-; \text{O}_2^-; \text{O}_3^-; \text{H}^+; \text{HO}_3 \end{aligned} \quad (26)$$

The expressions of the reaction rate for the different decomposition intermediates are the following:

$$r_{\text{HO}_2^-} = K_1 \cdot C_{\text{o},l}^* \cdot C_{\text{OH}^-,l}^* - K_2 \cdot C_{\text{o},l}^* \cdot C_{\text{HO}_2^-,l}^* \quad (27)$$

$$r_{\text{OH}^-} = -K_1 \cdot C_{\text{o},l}^* \cdot C_{\text{OH}^-,l}^* \quad (28)$$

$$r_{\text{O}_2^-} = K_2 \cdot C_{\text{o},l}^* \cdot C_{\text{HO}_2^-,l}^* - K_3 \cdot C_{\text{o},l}^* \cdot C_{\text{O}_2^-,l}^* \quad (29)$$

$$r_{\text{O}_3^-} = K_3 \cdot C_{\text{o},l}^* \cdot C_{\text{O}_2^-,l}^* + K_4^- \cdot C_{\text{HO}_3^-} - K_4^+ \cdot C_{\text{O}_3^-} \cdot C_{\text{H}^+} \quad (30)$$

$$r_{\text{H}^+} = K_4^- \cdot C_{\text{HO}_3^-} - K_4^+ \cdot C_{\text{O}_3^-} \cdot C_{\text{H}^+} \quad (31)$$

$$r_{\text{H}^+} = K_4^+ \cdot C_{\text{O}_3^-} \cdot C_{\text{H}^+} - K_4^- \cdot C_{\text{HO}_3^-} - K_5 \cdot C_{\text{HO}_3^-} \quad (32)$$

The mass balance of arsenic in the accumulation tank is described by the following total differential equation:

$$V_{\text{a,T}} \frac{dC_{\text{a,T}}}{dt} = F_l \cdot (C_{\text{a,T}}^{\text{in}} - C_{\text{a,T}}) \quad (33)$$

$$t = 0 \Rightarrow C_{\text{a,T}} = C_{\text{a,T}}(t=0)$$

where $V_{a,t}$ is the tank volume; $C_{a,T}^{in}$ and $C_{a,T}$ are, respectively, the inlet and outlet arsenic concentrations in the accumulation tank.

Model parameters

The different model parameters (K_L , K_m and K_g) were calculated using theoretical correlations described above. For this specific model the mass transport correlations can be written as follows:

$\underline{K_L}$

If $Re \geq 1.65$ then

$\underline{K_m}$

$K_m = 1.8 \cdot 10^{-3} \text{ m/s}$

$\underline{K_g}$

$K_g = 0.22 \cdot (F_g)^{1/3}$

$$K_L = 6.51 \cdot 10^{-5} \cdot e^{[4.2 + 0.4 \ln(F_l)]}$$

K_g (m/s); F_g (m³/s)

If $Re < 1.65$ then

$$K_L = 3.15 \cdot 10^{-5} \cdot e^{[12.6 + 1.2 \ln(F_l)]}$$

K_L (m/s); F_l (m³/s)

Model solution.

The model was implemented using the simulation software *ASPEN CUSTOM MODELER 11.1*.

Analysis of the operation variables.

By solving the implemented model the analysis of the operation variables has been carried out. For instance the influence of the flowrate, pH, temperature, etc. has been analysed. Table 2 shows the reference values of the variables in the model:

Table 2. Reference values of the variables in the model

Variable	Value
α	0,1
F_l	0.05 m ³ /h
F_g	0.1 m ³ /h
T_g	293 K
T_a	293 K
$[O_3]_{\text{initial}}$	5 mol/m ³
pH	7
V_{tank}	1 l
$[H_2O_2]$	$4 \cdot 10^{-3}$ M
$[As]_{\text{initial}}$	1 ppm

In all the cases the value of the variable under study is varied within a specific range, while the values of the other variables remain constant and equal to the reference values.

Influence of $\delta_r(\alpha)$

Figure 3 shows the evolution with time of the arsenic concentration in the tank for different values of α , that means different values of δ_r .

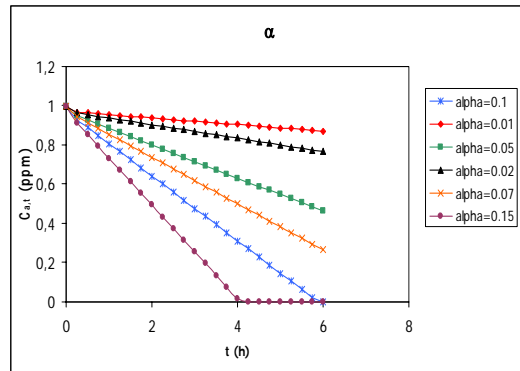


Figure 3. Influence of δ_r on the arsenic oxidation rate

The line in blue represents (in all the cases study) the simulation running with the reference values of the variables described in Table 2.

Analyzing the curves in Figure 3, it can be noticed that the higher value of α , the higher the oxidation rate. This behaviour is due to the fact that higher values of δ_r mean higher values of the reaction volume and consequently a faster reduction of the arsenic concentration.

δ_r is a model parameter and not an operation variable because its value depends on the system and not on the operation conditions. Therefore, the optimal value of α can be obtained by means of parameter estimation comparing experimental and simulated data.

Influence of F_I

Increasing the flowrate of the aqueous phase three phenomena take place in the system: i) a reduction of the residence time that means a lower reduction of the arsenic concentration, ii) a higher value of K_L , that means a lower mass transfer resistance in the aqueous phase stagnant layer, and iii) a lower value of δ_l and consequently a lower value of δ_r , thus reducing the reaction volume.

Figure 4 shows the evolution with time of the arsenic concentration in the tank for different values of the flowrate of the aqueous feed solution.

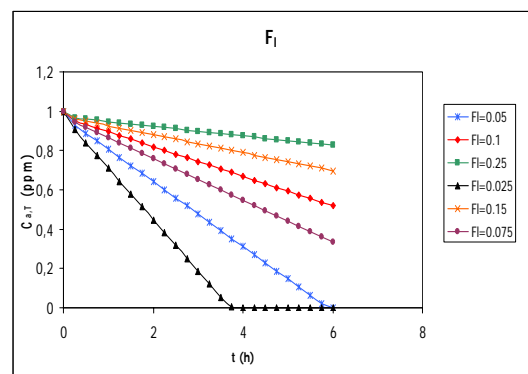


Figure 4. Influence of F_l on the arsenic oxidation rate

From Figure 4 it can be observed that increasing the aqueous phase flowrate, there is a lower reduction of the arsenic concentration. Therefore, the effect of the increased residence time, as well as the reaction volume, prevails on the reduction of the mass transfer resistance.

Influence of F_g

Figure 5 represents the evolution with time of the arsenic concentration in the tank for different values of the flowrate of the gaseous stream.

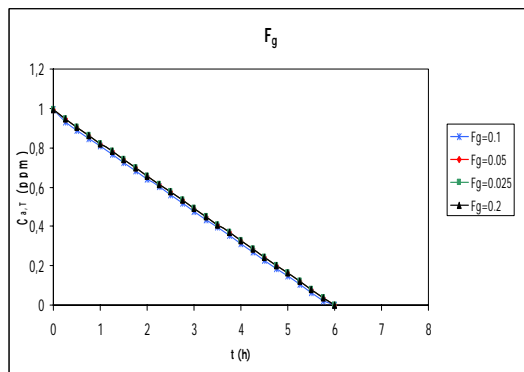


Figure 5. Influence of F_g on the arsenic oxidation rate

Analyzing Figure 5, it can be noticed that the influence of the gaseous stream flowrate can be considered negligible. This behaviour is owing to the fact that the gaseous stream flows continuously and always "fresh ozone" is supplied to the system. Moreover, the ozone concentration supplied is higher than the one stoichiometrically required for oxidizing arsenic.

Influence of T_g

Figure 6 represents the evolution with time of the arsenic concentration in the tank for different values of the gaseous stream temperature.

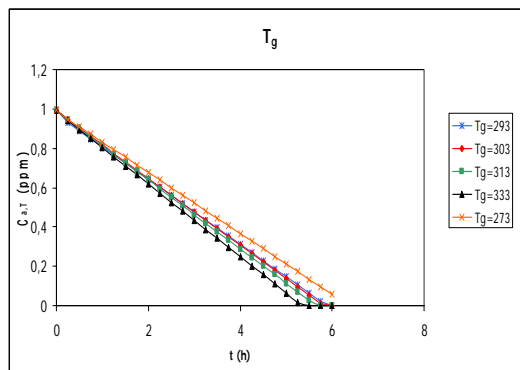


Figure 6. Influence of T_g on the arsenic oxidation rate

From Figure 6, it can be demonstrated that the influence of the gas temperature on the oxidation rate can be considered negligible.

Influence of T_l

Varying the temperature of the liquid phase, two opposite phenomena take place in the oxidation system: i) increasing the temperature, the value of the Henry's law constant decreases and consequently the ozone solubility is lower and, ii) the oxidation rate increases with the temperature. In relation to the variation of the kinetic constant with the temperature, there were not available data of the activation energy (E_a) for this system and consequently it was not possible to take into account the temperature contribution to the oxidation rate. Therefore, the mathematical model is only able to take into account the influence of the liquid phase temperature in the Henry's law constant.

Figure 7 represents the evolution with time of the arsenic concentration in the tank for different values of the liquid phase temperature.

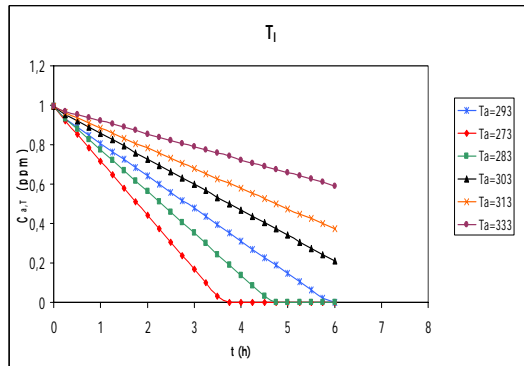


Figure 7. Influence of T_l on the arsenic oxidation rate

As it was expected, the higher the temperature, the lower the Henry's law constant and thus a lower oxidation rate because of the lower concentration of ozone in the liquid phase.

Influence of the initial ozone concentration

Figure 8 represents the evolution with time of the arsenic concentration in the tank for different values of the initial ozone concentration.

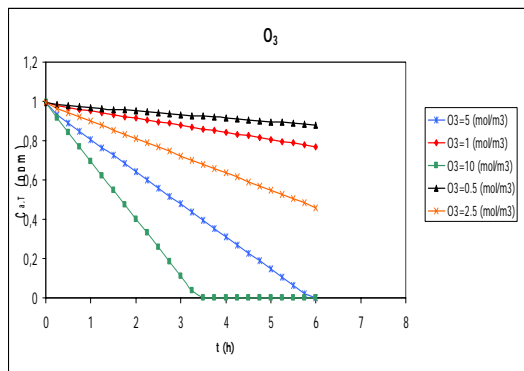


Figure 8. Influence of initial ozone concentration the arsenic oxidation rate

From Figure 8 it can be noticed that increasing the ozone concentration the oxidation rate also increases. This behaviour is explained by the low ozone solubility in aqueous solutions. This step can be considered the limiting factor of the oxidation process and thus considering the mass transfer resistance in the gaseous phase negligible. For this reason, the ozone concentration that reaches the gas-liquid interface is similar to the ozone concentration in the bulk. Therefore, if the ozone concentration in the bulk increases, the ozone concentration in the interface will be higher and consequently a higher amount of ozone will be dissolved in the aqueous phase increasing the oxidation kinetics.

Influence of V_{a,T}

Figure 9 shows the evolution with time of the arsenic concentration in the tank for different values of the aqueous phase recycling tank.

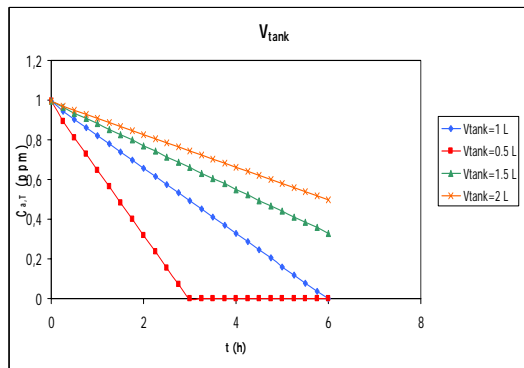


Figure 9. Influence of V_{a,T} on the arsenic oxidation rate

Lower volumes to be treated, at parity of initial arsenic concentration, mean a lower time needed to achieve the total oxidation.

Influence of pH

The pH of the aqueous phase solution has influence on the system in two different ways:

- i) In the Henry's law constant. From Eq.(17) it can be seen that increasing the pH, the value of the Henry's law constant is higher and consequently the oxidation rate increases.
- ii) In the rate of ozone decomposition. From Eq.(1) it can be seen that OH⁻ are taking part in the ozone decomposition. Increasing the pH, the concentration of OH⁻ increases and consequently the rate of the initiation reaction in the ozone decomposition is higher. This is true working with solutions without H₂O₂ where the initiation of ozone decomposition only takes place by means of reaction (1). If hydrogen peroxide is present, the reaction between O₃ and OH⁻ can be considered negligible (low value of K₁) and the initiation of ozone decomposition can be described by reaction (2) (high value of K₂).^{15,18} Therefore, analysing the overall decomposition mechanism (reactions (2) to (6)) it can be noticed that decreasing the pH the H⁺ concentration increases and consequently reaction (4) is shifted to the right increasing the rate of the ozone decomposition.

Figure 10 shows the evolution with time of the arsenic concentration in the tank for different values of pH of the aqueous phase.

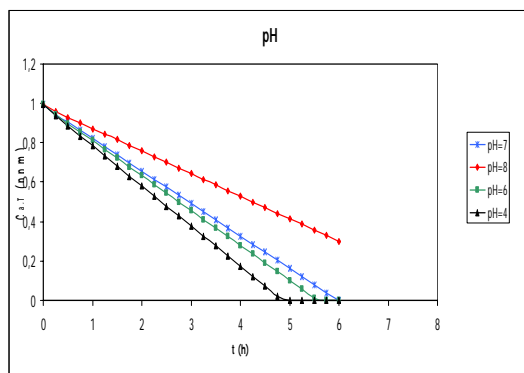


Figure 10. Influence of pH on the arsenic oxidation rate

From Figure 10 it can be noticed that decreasing the pH the arsenic oxidation rate increases. Analysing the overall behaviour of the system it can be said that the influence of pH on the reaction mechanism is more important than the influence on the Henry's law constant.

Influence of the initial H₂O₂ concentration

Figure 11 shows the evolution with time of the arsenic concentration in the tank for different values of the initial concentration of hydrogen peroxide.

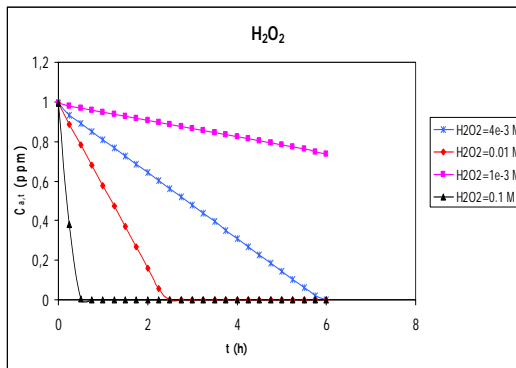


Figure 11. Influence of initial $[H_2O_2]$ on the arsenic oxidation rate

By adding a certain amount of H_2O_2 to the system the reaction rate increases (see Figure 11). This behaviour is owing to the fact that hydrogen peroxide is dissociated in water, following the reaction in Eq.(6). Then, the HO_2^- anions formed as consequence of the dissociation step can react with ozone initiating the ozone decomposition as was shown in Eq.(2).

Influence of the initial arsenic concentration

Figure 12 shows the evolution with time of the arsenic concentration in the tank for different values of the initial arsenic concentration in the aqueous feed solution.

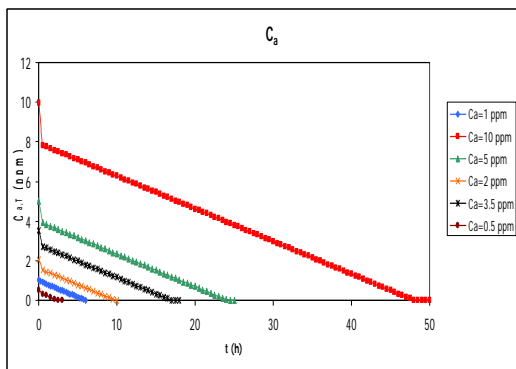


Figure 12. Influence of initial $[As]$ on the arsenic oxidation rate

From Figure 12 it can be observed that all the curves have the same slope and for this reason the oxidation rate is the same independently on the initial arsenic concentration. The only difference is that in solutions with higher arsenic concentration the time required for the total oxidation is higher.

Further work

In relation to further work different aspects should be considered:

Model Validation.

It is necessary to validate the model in order to know if there is a good agreement between experimental and simulated data. In this point two possible solutions can be considered:

- i) To analyze the experimental data obtained by EPA²⁵. The experimental set up used in this work is not based on membranes and, therefore, we can compare the experimental data obtained by these authors with the ones obtained by simulation in order to know if there is some improvement in the oxidation step working with a membrane contactor.
- ii) To make the model validation with the experimental results that will be obtained at the ITM-CNR laboratory for the arsenic oxidation by membrane contactors using air/oxygen. In this way, we have to modify the model parameters in order to take into account the properties of the new oxidant and the new kinetic expression.

Model improvement.

If there is no a good agreement between experimental and simulated data some changes in the model hypothesis and model parameters should be done. These changes could include a more exhaustive description of the process.

Coupling between the pre – treatment (oxidation) and the RO or NF step.

If would be a good idea to develop a model that allows describing the different parts of the process: the pre – treatment and the pollutant removal by RO or NF technology.

References

1. Emeet, M. T.; Khoe, G. H. Photochemical oxidation of arsenic by oxygen and iron in acidic solutions. *Wat. Res.* 35(3), 649 – 656, **2001**.
2. Ning R. Y. Arsenic removal by reverse osmosis. *Desalination*. 143, 237-241, **2002**.
3. Borho, M.; Wilderer, P.; Optimized removal of arsenate (III) by adaptation of oxidation and precipitation processes to the filtration steps. *Wat. Sci. Tech.* 34(9), 25-31, **1996**.
4. Robins, R. G.; Nishimura, T.; Singh, P. Removal of arsenic from drinking water by precipitation, adsorption or cementation. Ahmed, M. F.; Ali, M.A.; Adeel, Z., eds. Technologies for Arsenic Removal from Drinking Water. Tokyo; Dhaka: The United Nations University; Bangladesh University of Engineering and Technology; 31-42. **2001**.
5. Bissen, M.; Frimmel, F. H. Arsenic a review. Part II: Oxidation of arsenic and its removal in water treatment. *Acta. Hydrochim. Hydrobiol.* 31(2), 97-107, **2003**.
6. Kang, M.; Kawasaki, M.; Tamada, S.; Kamei, T.; Magara, Y. Effect of pH on the removal of arsenic and antimony using reverse osmosis membranes. *Desalination*. 131, 293-298, **2000**.
7. Floch, J.; Hideg, M. Application of ZW – 1000 membranes for arsenic removal from water sources. *Desalination*. 162, 75-83, **2004**.
8. Moore, K. Treatment of arsenic contaminated groundwater using oxidation and membrane filtration. *PhD thesis*. University of Waterloo. Waterloo, Ontario (Canada), **2005**.
9. Shih, M. C. An overview or arsenic removal by pressure driven membrane processes. *Desalination*. 172, 85-97, **2005**.
10. Kim, M. J.; Nriagu, J. Oxidation of arsenite in groundwater using ozone and oxygen. *Sci. Total. Environ.* 247, 71-79, **2000**.
11. Driehaus, W.; Seith, R.; Jekel, M. Oxidation of arsenate (III) with manganese oxides in water treatment. *Wat. Res.* 29(1), 297-305, **1995**.
12. Pettine, M.; Campanella, L.; Millero, F. J. Arsenite oxidation by H₂O₂ in aqueous solutions. *Geochim. Cosmochim. Acta*. 63(18), 2727-2735, **1999**.

- [13. Kenson Associates. Report on practical methods for removal of arsenic from subsurface aquifers and drinking water systems, **2006**. Internet: <http://www.environmental-expert.com>
- [14. Baudot, A.; Floury, J.; Smorenburg, H. E. Liquid – Liquid extraction of aroma compounds with hollow fiber contactors. *AIChE J.* 47(8), 1780-1793, **2001**.
- [15. von Gunten, U. Ozonation of drinking water: Part I. Oxidation kinetics and product formation. *Wat. Res.* 37, 1443-1467, **2003**.
- [16. Hoigné, J.; Bader, H.; Haag, W. R.; Staehelin, J. Rate constants of reactions of ozone with organic and inorganic compounds in water – III. Inorganic compounds and radicals. *Wat. Res.* 19(8), 993 – 1004, **1985**.
- [17. Buxton, G. V.; Greenstock, C. L.; Helman, W. P.; Ross, W. P. Critical review of rate constants for reactions of hydrated electrons, hydrogen atoms and hydroxyl radicals in aqueous solution. *J. Phys. Chem. Ref. Data.* 17, 513-886, **1988**. Internet: <http://allen.rad.nd.edu>.
- [18. Staehelin, J.; Hoigné, J. Decomposition of ozone in water: Rate of initiation by hydroxide anions and hydrogen peroxide. *Environ. Sci. Technol.* 16, 676-681, **1982**.
- [19. Gordon, G. The chemistry and reactions of ozone in our environment. *Prog. Nucl. Energ.* 29, 89-96, **1995**.
- [20. Sengupta, A.; Peterson, P. A.; Miller, B. D.; Scheneider, J.; Fulk Jr., C. W. Large – scale application of membrane contactors for gas transfer from or to ultrapure water. *Separ. Purif. Techn.* 14, 189-200, **1998**.
- [21. Criscuoli, A.; Drioli, E.; Moretti, U. Membrane contactors in beverage industry for controlling the water gas composition, in *Advanced Membrane Technology*, editors: E. Drioli, G.G. Lipscomb, and W.S.W. Ho, *Annals of New York Academy of Sciences*, New York, USA 984, 1-16, ISBN: 1-57331-427-7, **2003**.
- [22. USEPA. Arsenic removal from drinking water by ion exchange and activated alumina plants. EPA/600/R-00/088, **2000**.
- [23. Jansen, R. Ozonation of humic substances in a membrane contactor. Mass transfer, product characterization and biodegradability. *PhD thesis*. University of Twente. Enschede (The Netherlands), **2005**.
- [24. Wickramasinghe, S. R.; Semmens, M. J.; Cussler, E. L. Mass transfer in various hollow fiber geometries. *J. Memb. Sci.* 69, 235, **1992**.
- [25. USEPA. Laboratory study on the oxidation of arsenic III to arsenic V. EPA/600/R-01/021, **2001**.

A3. Contenidos del Formato Electrónico de la Tesis Doctoral

En el formato electrónico de la Tesis Doctoral (formato CD) se adjunta la siguiente información:

- Memoria de Tesis Doctoral en formato PDF.
- Artículo: "Ortiz, I., San Román, M.F., Corvalán, S.M., Eliceche, A.M. (2003), Modeling and Optimization of an Emulsion Pertraction Process for Removal and Concentration of Cr(VI), *Ind. Eng. Chem. Res.*, 42(23), 5891-5899" (Formato PDF).
- Carpeta con las hojas de seguridad (HD) de los diferentes reactivos empleados en la experimentación (Formato PDF). Los archivos incluidos son los siguientes:
 - HD del Alamine 336
 - HD del Ácido Sulfúrico
 - HD del Cloruro Sódico
 - HD del Cromato Sódico
 - HD del 1-Dodecanol
 - HD del Hidróxido Sódico
 - HD del Isopar-L
 - HD del Pluronic PE3100
 - HD del Sulfato Sódico
- Carpeta con los programas de gPROMS (modelado matemático) y GAMS (optimización matemática) en formato PDF.
- Carpeta con información relativa a la difusión de resultados. En esta carpeta se recogen los artículos y comunicaciones a congresos (formato PDF) listados en el Anexo A.1.